Modeling the Effect of Magnetoelectric Nanoparticles on Neuronal Electrical Activity: An Analog Circuit Approach

Zeinab Ramezani[1], Victoria André[2], Sakhrat Khizroev[3]*

Abstract

This paper introduces a physical neuron model that incorporates MagnetoElectric NanoParticles (MENPs) as an essential electrical circuit component to wirelessly control local neural activity. Availability of such a model is important because MENPs, due to their magnetoelectric effect, can wirelessly and non-invasively modulate neural activity, which in turn has implications for both finding cures for neurological and other diseases and creating a high-resolution wireless non-invasive brain-machine interface. When placed on a neuronal membrane, MENPs act as magnetic-field-controlled finite-size electric dipoles that generate local electric fields across the membrane in response to magnetic fields, thus allowing to controllably activate local ion channels, in turn locally initiating an action potential. Herein, the neuronal electrical characteristic description is based on ion channel activation and inhibition mechanisms. A MENP-based memristive Hodgkin-Huxley (MMHH) circuit model is extracted by combining the Hodgkin-Huxley (HH) model and an equivalent circuit model for a single MENP. In this model, each MENP becomes an integral part of the neuron, thus enabling a wireless local control of the neuron's electric circuit itself. Furthermore, the model is expanded to include multiple MENPs to describe collective effects in neural systems.

Keywords Magnetoelectric nanoparticles, Brain-machine interface, Neuronal electrical activity, Analog circuit modeling.

I. Introduction

An open issue remains in neuroscience regarding the capability to wirelessly stimulate specific local regions in central and peripheral nervous networks (CNS and PNS) in a controlled manner without using invasive procedures such as surgically implanted electrodes or genetic modification [1, 2]. One promising solution is to use MagnetoElectric NanoParticles (MENPs) [1, 3, 4]. MENPs, made of materials exhibiting strong coupling between magnetic and electric fields, display a relatively strong magnetoelectric (ME) effect, thus allowing for a local conversion of a magnetic field into dipole electric fields [5, 6]. As a result, if placed on the cellular membrane, MENPs can serve as wireless alternating current (a.c.) nanoelectrodes which are controlled via application of an a.c. magnetic field [4]. Given each MENP is a finite-size electric dipole with a characteristic size on the order of the membrane thickness, the electric field by each pole of the dipole can be sufficiently strong to significantly affect the local membrane potential in the immediate vicinity of the pole.

[1] Department of Electrical and Computer Engineering, College of Engineering, University of Miami, Miami, FL, USA.
ORCID: 0000-0003-0228-1283
[2] Department of Biomedical Engineering, College of Engineering, University of Miami, Miami, FL, USA.
[3] Department of Electrical and Computer Engineering, College of Engineering, University of Miami, Miami, FL, USA.
ORCID: 0000-0002-4299-7094
*Corresponding author: skhizroev@miami.edu

Obviously, the nanoparticles would not produce significant effects if they were not placed directly on the dielectric membrane and instead are located in either intracellular or extracellular spaces. With the two spaces being conductive, the electric field generated in any point within the spaces would be screened out by free moving ions [7-11]. Thereby, given an adequate density of MENPs on the membrane surface in a local region, the simultaneously accumulated energy of the nanoparticles in the region can be large enough to induce a local action potential. In other words, by generating local action potentials deep in the brain via application of magnetic fields, MENPs offer a wireless alternative to existing local deep-brain stimulation (DBS) approaches that use surgically implanted electrodes. Ideally, since their spatial resolution is limited only by the nanoparticle size and the ability to control spatiotemporal patterns of the remotely applied magnetic field, MENPs could wirelessly activate action potentials on demand in a single neuron [12-15]. Also, in contrast with transcranial magnetic stimulation (TMS) systems, MENPs don't need relatively large brain volumes and rapidly changing (<<1msec) high magnetic fields (~1T) to generate sufficiently strong eddy currents [16]. Instead, the required local stimulation control is achieved by application of relatively small fields (<<1T) in a wide frequency range [12]. This fundamental difference is due to the fact that MENPs, when placed on the membrane, become an integral component of the neuron, which in turn provides this novel wireless and non-invasive control of local activity of the associated neural circuits. However, to fully take advantage of this important MENPs-based external control it is critical to understand the complex electric-field interaction between MENPs and neural circuits. It is worth noting that the MENPs' magnetoelectric effect enables a two-way interaction with the circuits: (i) applying external magnetic fields to control local

intrinsic electric fields, thus providing local modulation of neural activity in the nanoparticles' vicinity and (ii) converting local electric fields due to local neural activity into the nanoparticles' magnetization change, which in turn can be detected via external magnetometers, thus enabling a one-of-a-kind mechanism to wirelessly record local neural activity [17], breaking the current stalemate in the field of neural recording due to the inverse mathematics problem [https://doi.org/10.1186/1743-0003-5-25].

Again, for this two-way interface to work, it is difficult to underscore the importance of ensuring the nanoparticles are brought into direct contact with the neuronal membrane. Otherwise, the local electric field induced or sensed by the nanoparticles undergoes an overwhelming screening by free ions in the conductive microenvironment, thus rendering MENPs largely ineffective. The characteristic screening scale, known as the Debye length [18], plays a crucial role in determining the extent to which charged particles can interact with and penetrate biological membranes [19]. This length scale arises from the balance between the thermal energy of ions and their electrostatic interactions with the surrounding medium.. Classic works by Alberts et al. [18], Hille [19], Hodgkin and Huxley [20], and Neher and Sakmann [21] provide foundational insights into the concept of the Debye length and its implications for electrostatic interactions at biological interfaces.

There have been several research efforts on modeling diverse neurons using either biophysically detailed or point neuron models [22-24]. These studies focus on the neocortex, a crucial region of the mammalian brain responsible for functions such as perception, memory, intelligence, and consciousness [25]. Moreover, such modeling efforts have been instrumental in discussing various diseases, [26] and shedding light on the mechanisms underlying neuronal activity and computations [27]. With MENPs showing promising potential for biomedical applications, including improving the effectiveness of cancer treatments, enhancing imaging techniques, and developing new therapies for neurological diseases [4, 28-31], modeling MENPs as a circuit can provide a useful framework for understanding the behavior of these nanoparticles and predicting their properties. Specifically, the circuit model can help describe the complex interplay between magnetic and electric fields in these nanoparticles.

One approach to quantify the MENPs-neuron circuit interaction is to create a circuit model that describes the interplay between the nanoparticles' magnetic and electric fields in actual neural systems. Such a circuit model can help gain insight into the nanoparticles-based effects on neural circuits depending on the nanoparticles' size, shape, and composition as well as the strength and frequency of the applied magnetic and generated electric fields. In turn, the model can help predict the nanoparticles' effects on and, reciprocally, response to different stimuli in actual neural systems.

II. Equivalent Circuit Model to Simulate Nanoparticles' Effects on the Nervous System

In this study, the effects of magnetic and electric fields are represented through effective currents and voltages, with each MENP modeled as a circuit element with specific electrical properties. An analog circuit is created based on the MENP-neuron interaction. In order to lay down a solid foundation for the model, we will first explain the Hodgkin-Huxley (HH) model and its associated equations. Then, a single-MENP circuit is proposed, with the circuit later expanded to include thousands of MENPs. Finally, a theory regarding the effect of MENPs on neurons will be presented, and two circuit models based on the theory will be discussed.

A. Hodgkin-Huxley model

Neurons are classified as electrically excitable cells that use electrochemical signaling to process and transmit information [32]. The communication between neurons is made possible through synapses, which transmit electrochemical signals from one neuron to another in the form of neurotransmitters, thereby establishing a series of connections among neurons in neuronal networks [33]. For successful chemical synaptic transmission in biological neurons, various processes are crucial [34, 35]. A high-level illustration of initiation, propagation and termination of a collective neural activation known as an Action Potential (AP) is shown in Fig. 1a. The traditional representation of the microstructure of a single neuron, with all the conventional terminology used to define all the key neuron's parts, is shown in Fig. 1b. The dynamic of the membrane potential during the three AP states, besides the main rest state, including depolarization, repolarization and hyperpolarization, respectively, is shown in **Fig. 1c.**

Biophysical models of neurons and synapses refer to mathematical models that aim to describe the physical properties and behavior of neurons and synapses based on biophysical principles [36]. These models take into account the cellular and molecular mechanisms underlying the generation and transmission of electrical signals in the nervous system and are essential for understanding the complex dynamics of neural circuits [20]. Hodgkin and Huxley developed the first biophysical model of action potential generation in neurons, based on their experiments with the giant axons of squid [20]. The Hodgkin-Huxley (HH) model describes the electrical behavior of neurons and is based on ion channel activation and inactivation principles [37]. The conductive cytoplasm that makes up the ionic fluids can be found inside and outside the dielectric membrane. The dielectric membrane separates the two conductive domains known as the intracellular (cytosol) and extracellular spaces, respectively. In other words, the axon membrane acts as a barrier between the two fluids (conductors) inside and outside the cell membrane. The capacitor is the representation of the charge storage capacity that is created when an insulator is placed between two conductors. The region of the axon membrane that does not contain ion channels can be thought of as a capacitor (C_m). The lipid bilayer, the membrane protein, and the ion channels make up the components that make up the axon membrane of the neuron (**Fig.1**).

According to this model, two nonlinear conductances, denoted by the symbol g_{Na} and g_K, are used to represent the sodium and potassium ion channels, respectively. Other ion channels are described as having a linear conductance (g_L) [38]. Therefore, the model is made up of three major ion channels including sodium (Na^+), potassium (K^+), and leak (L) channels,

respectively, each with its own conductance (g_{Na}, g_K, and g_L) and reversal potential (E_{Na}, E_K, and E_L). Furthermore, the model introduces three variables called "gating" variables m, n and h, respectively, to describe the probability of each channel to be open at a given time. The sodium channel is controlled by the combined action of m and h, the potassium channel is controlled by n. The following voltage-current equations are derived from a mathematical analysis of the RC equivalent circuit (**Fig.2 (a)**).

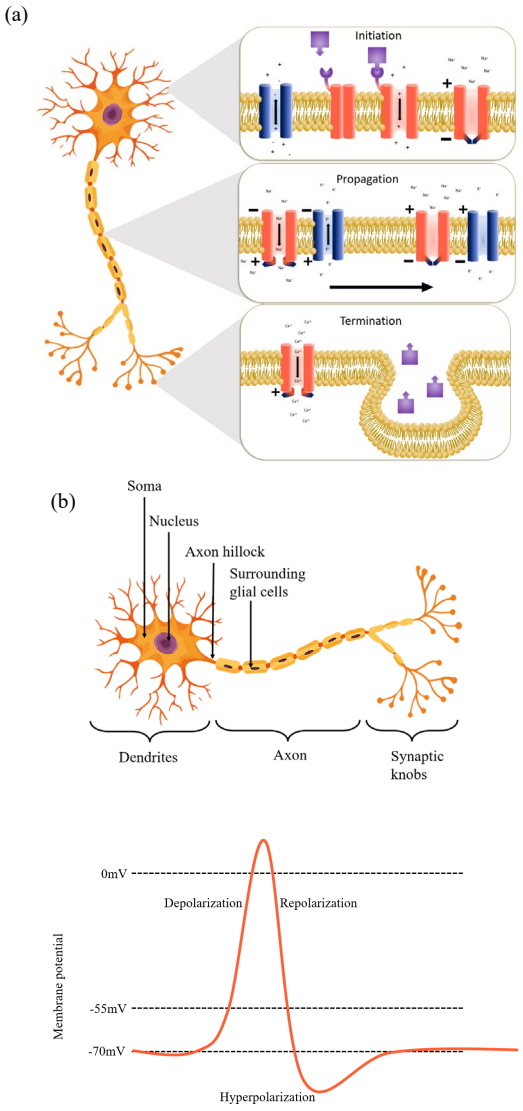

Fig.1. (a) Schematic of initiation, propagation, and termination of a collective neuronal firing event. (b) Labeled diagram of a stereotypical neuron. (c) Membrane potential profile initiated by an action potential.

The equations governing the behavior of the HH model are shown below [20]:

$$C_m\left(\frac{dV(t,x)}{dt}\right) = I_{ext}(t,x) - g_{Na}(V-V_{Na}) - g_K(V-V_K) - g_L(V-V_L) + \frac{1}{(2r_{in})\partial^2 V(t)/\partial^2 x} \quad (1)$$

$$g_{Na} = g_{NaMax}m^3h, g_K = g_{KMax}n^4, g_L = g_{LMax}, \quad (2)$$

where $I_{ext}(t,x)$ is the external current input to the neuron, and C_m is the membrane capacitance. The maximum values of potassium, sodium, and leaky conductances are denoted by g_{KMax}, g_{NaMax}, and g_{LMax}, respectively. Their typically measured values would be 36, 120, and 0.3 Ohm^{-1} cm^{-2}, respectively [20]. The reversal potentials for the sodium, potassium, and leak channels are E_{Na} = 115 mV, E_K = -12 mV, and E_L = 10.6 mV, respectively.

For practical purposes, these equations are best written in the form: V = E-E_r, V_{Na} = E_{Na} -E_r, V_K=E_K-E_r, V_L=E_i-Er. Here, E_r is the absolute value of the resting potential. V, V_{Na}, V_K and V_L are then directly measured as displacements from the resting potential. The last term in **Eq. (1)** is the rate of charge along the inside surface of the membrane in the direction of the current. It only depends on time, t, rather than location, x, so the quadratic partial differential term is equal to zero. Therefore, **Eq. (1)** can be rewritten as:

$$C_m\left(\frac{dV(t,x)}{dt}\right) = I_{ext}(t,x) - g_{Na}(V-V_{Na}) - g_K(V-V_K) - g_L(V-V_L) = I_{ext}(t,x) - I_{ion}(t,x) \quad (3)$$

And the gating variables (m, h, and n) are governed by the following equations [20]:

$$\frac{dm}{dt} = \alpha_m(1-m) - \beta_m m \quad (4)$$

$$\alpha_m = \big(0.1(V+25)\big)/\left(\left(\frac{\exp(V+25)}{10}\right)-1\right), \quad \beta_m = 4exp(V/18),$$

$$\frac{dh}{dt} = \alpha_h(1-h) - \beta_h h \quad (5)$$

$$\alpha_h = 0.07exp(V/20), \beta_h = \frac{1}{1+exp\left((V+35)/10\right)},$$

$$\frac{dn}{dt} = \alpha_n(1-n) - \beta_n n \quad (6)$$

(c)
$$\alpha_n = \big(0.01(V+10)\big)/\left(\left(\frac{\exp(V+10)}{10}\right)-1\right)), \quad \beta_N = 0.125exp(V/80)$$

The transition rate α describes how quickly ion channels change from closed to open. The transition rate β indicates how quickly ion channels change from open to closed. α and β are rate constants that change with voltage but not with time and have dimensions of [time]$^{-1}$. The above defined variables n, m, and h are dimensionless variables which vary between 0 and 1 [20].

It was found that increasing the conductance of the sodium channel would raise the membrane potential, which would cause the first spike in the action potential [39]. In addition, **Eq. (3)** shows that (V-V_{Na}) is a negative number, so if I_{ext} stays the same and the conductance goes up, C_m (dv/dt) will go up as well. The m and h gates of the sodium channel control how much sodium moves through the channel. At first, m = 0, so the conductance of the sodium channel is zero, and dm/dt = α_m. This means that after the first spike of the action potential, m will go up until it equals 1. At that point, dm/dt = β_m, and the sodium channel's conductance will go down. This means that the membrane potential will also go down. In the same way, one can look at how the potassium channel affects how the action potential is made. If the potassium channel's conductance went up, the membrane potential would go down. Also, **Eq. (3)**

shows that ($V - V_K$) is a positive number, so if I_{ext} stays the same and ($V-V_K$) goes up, C_m (dv/dt) will go down. The channel gate n controls how much the potassium channel lets ions pass through it. Based on [39], at first, n = 0, so the potassium channel conductance is also 0. Since $dn/dt = \alpha_n$, n will go up after the first spike of the action potential until it reaches 0.7. At that point, β_n will be more important than α_n, so n will go down. This will cause the conductance of the potassium channel to go down, which will cause the membrane potential to go up. The refractory period in the generated action potential is caused by this increase.

Due to the complexity of the HH model, various other models that aim to simplify the neuron action potential have been proposed such as memristive HH(MHH) [39]. A memristor is any two-terminal device whose instantaneous current and voltage should follow Ohm's law, which changes depending on the state of the device [40] and its I–V characteristic should meet three conditions, (i) the zero crossing property, (ii) the pinched hysteresis loop, and (iii) the frequency-dependent pinched hysteresis property [41]. Based on Chua's interpretation of the HH model [41] and the [39], **Fig. 2(b)** could show the simplified neuron model and the MHH circuit model, since the sodium and potassium channels have been shown to be generic memristors which can remember and change its resistance based on the charge that passes through it [42]. The MHH model includes two additional memristive variables that represent the state of a memristive device that modulates sodium and potassium channel conductance. The conductance, or ability to allow ions to pass through, of sodium and potassium channels is modulated by the membrane potential and the history of ion flow (channel activation and inactivation)[43]. The conductance of these channels changes as the membrane potential changes, forming a relationship between the charge (ion flow) and the flux linkage (membrane potential).

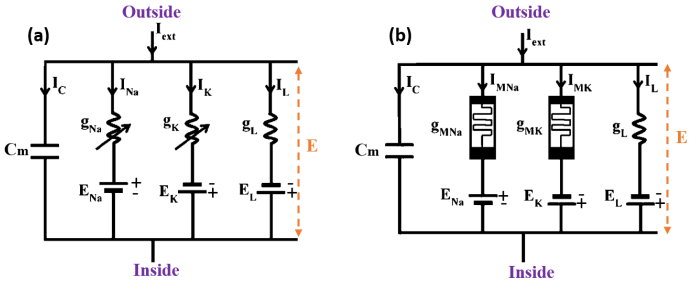

Fig. 2. Electrical circuit representing axon cell membrane (a) HH circuit model (b) MHH circuit model.

The memristor equation can be used to explain the memristive behavior of sodium and potassium channels as below[44, 45]:

$$M(q(t)) \times i(t) = V(t) \tag{7}$$

The voltage (V) in this equation represents the membrane potential, the current (i) the flow of ions, and M(q(t)) the memristance, which captures the relationship between charge and flux linkage.

B.Modeling MENPs as Circuit Elements and their Effect on Neurons

In this study, in order to create a circuit model of MENPs, key circuit parameters are modified to take into account the contributions from the magnetostrictive and piezoelectric coupling in the nanoparticles when a magnetic field is applied. The magneto-elasto-electric equivalent circuit for such magnetoelectric composite nanoparticles is shown in **Fig. 3.**

The circuit includes a coupling factor (ϕ_m) that transforms the external magnetic field (H) into a mechanical voltage ($\phi_m H$), and a transformer (ϕ_p) that represents the electromechanical coupling in the circuit. Mechanical and electric currents are denoted as I_1 and I_2, respectively, while applied magnetic field and induced voltage are represented by H and V'.

The ME voltage coefficient, which is the ratio of an induced electric field to an applied magnetic field, is a crucial parameter for Direct-ME. Using Kirchhoff's voltage and current laws along with the equivalent circuit and transformer, the ME voltage coefficient $\alpha_E(\omega)$ obtained as a function of the A.C. magnetic-field frequency as below:

$$\alpha_E(\omega) = \frac{\partial V'}{\partial H} = \frac{\varphi_m}{\left(\frac{(Z_L llZ) + C_c}{Z_L llZ}\right)\varphi_p + \left(\frac{Z_M}{(Z_L llZ)\varphi_p}\right)} \tag{8}$$

$$Z_{th} = \left(\frac{Z_m}{{\varphi_p}^2} - \frac{1}{jc\omega}\right) ll\ (Z_L llZ) \tag{9}$$

$$V_{th} = H - \left(\frac{Z_m}{\varphi_p \varphi_m} \times \frac{V'}{Z_L llZ}\right) \tag{10}$$

$$I_{th} = \frac{V_{th}}{Z_{th}} \tag{11}$$

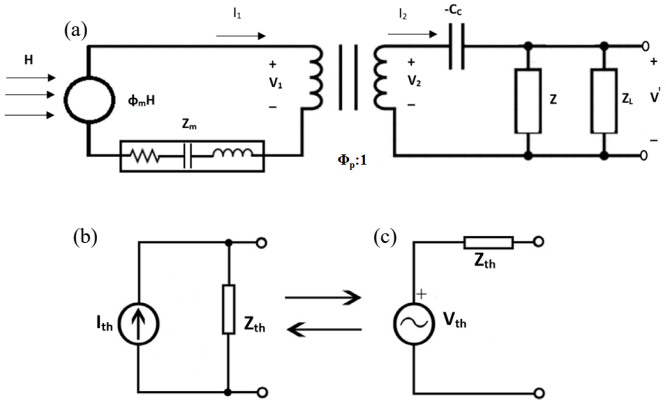

Fig. 3. (a) Magnetoelectric equivalent circuit with added bioload as an impedance. (b) Norton's equivalent circuit. (c) Thevenin's equivalent circuit.

The frequency response is an intrinsic property of these nanoparticles. At resonant frequencies, e.g., in the gigahertz range, the magnetoelectric coefficient could be increased by order of magnitude. Therefore, this property can be taken into account to select a way to transmit/receive energy carried by magnetic fields. Indeed, magnetic fields at resonant frequencies could be useful as carriers of the energy, while neural activity at substantially lower frequencies modulating the transmitted/received signal. Therefore, The frequency of the

applied magnetic field is a crucial parameter that governs the dynamics of the magnetoelectric effect, influencing the activation of neurons by modulating electric field variations across the neuronal membrane. The frequency of the magnetic field can affect the extent of MENPs' polarization and the generation of local electric fields across the membrane. This, in turn, modulates the activation of ion channels and influences the flow of ions across the membrane, ultimately impacting neuronal excitability and firing patterns.

To model the effect of thousands of MENPs on neurons, it is necessary to consider the collective behavior of the nanoparticles as they interact with all the neurons in the system. This can be done by combining a circuit analysis and a biophysical modeling. Firstly, the described equivalent circuit for a single MENP should be expanded into an equivalent circuit for a population of nanoparticles. This can be accomplished by viewing the nanoparticles as a series of parallel circuits, with each circuit representing a single nanoparticle. Again, it is noteworthy that this approximation holds true only if the nanoparticles are in direct contact with the (dielectric) membrane region. Otherwise, if they are in the conductive intracellular or extracellular spaces, i.e., not in direct contact with the dielectric membrane, their fields would be rapidly (within a millisecond time scale) screened out by free moving ions in the two coductive spaces, with a characteristic screening scale defined by the Debye length, known to be in the sub-1-nm range [7]. Also, obviously, no physical current can flow through the nanoparticles because they are dielectric. Therefore, this model would work best in the typical alternating current (a.c.) case. **Fig. 4** shows an equivalent circuit for a population of nanoparticles. Using Kirchhoff's current law, the total effective current flowing through the population of nanoparticles can be calculated as follows:

$$I'_{th} = \sum_{k=0}^{n} I_{thk} \tag{12}$$

Also, the Z_{th} can be written as:

$$Z'_{th} = Z_1 llZ_2 llZ_3 \dots\dots\dots\dots llZ_n \tag{13}$$

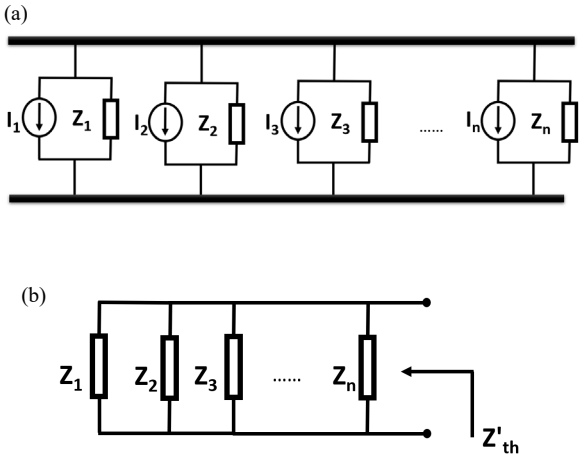

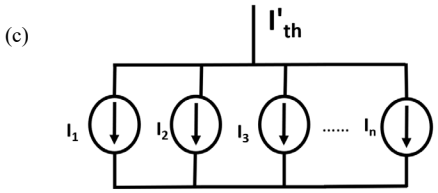

Fig. 4. (a) An equivalent circuit for the entire population of nanoparticles (b)Total Impedance (c) Total Effective current.

Theory of MENPs Effect on Neurons and Proposed Circuits Models

Neural activity is a complex process involving the interaction of numerous factors such as ion channels, neurotransmitter levels, and the properties of the synapses that connect neurons to other cells in the network. These factors ultimately control the excitability of neurons and the rate at which they fire. Dynamical analysis and synchronization transitions have been extensively studied on numerous neuron models, and it has been established that the modes of electrical activities can be altered by external forcing current [46-48]. This has resulted in the development of a number of methods for modulating neuronal activity, including the use of MENPs [3, 13].

As mentioned above, MENPs are integrated into neural circuits to provide an external field control to locally activate neurons. When attached to the neuronal cell membrane, these nanoparticles act as magnetic-field-controlled electric dipoles, generating local a.c. electric fields across the membrane upon application of a.c. magnetic fields, resulting in neural firing [12, 49]. When a magnetic field is applied across the membrane, the induced (due to the ME effect) internal electric field of the nanoparticle, i.e., the polarization (dipole moment per unit volume), leads to modifying the equilibrium state, in turn leading to moving ions across the membrane. In other words, MENPs become an integral part of the membrane, thus allowing to wirelessly control of the local membrane potential, in turn leading to local neural activation. This is based on the unique properties of MENPs, particularly their ability to act as magnetic-field-controlled electric dipoles. With no MENPs in the system, the charge distribution around the membrane is determined by the energy equilibrium that takes into account chemical and physical forces. In the equilibrium, there is a non-zero voltage (membrane potential) formed across the membrane. Hence, this implies that the electric field generated across the membrane is an important factor that determines the force balance in the equilibrium. When MENPs are positioned on the neuronal membrane and subjected to external magnetic fields, they generate additional local electric fields across the membrane. In turn, these electric fields change the above force balance, thus modifying the equilibrium. In this respect, these nanoparticles become an integral part of the membrane. Indeed, in this arrangement, MENPs directly influence the activity of ion channels embedded in the membrane, thereby affecting

neuronal excitability and signaling, which is the purpose of the membrane. Such local activation depends on the nanoparticles' ME effect, the relative location with respect to the membrane surface and the nanoparticles' density. It can be argued that for optimal results, a nanoparticle must be positioned at the membrane in a symmetrical position with respect to the membrane. For example, the position at which a MENP interfaces with the membrane so that its volume remains in the extracellular space is shown in Fig. 5a. In this case, the electric field due to the MENP's dipole can be significantly higher because the dipole's pole is right on the membrane. The actual field can be easily estimated from Coulomb's law and depends on the ratio of the dipole length to the thickness of the membrane. For comparison, given the dipole length and the membrane thickness on the order of 30 and 10 nm, respectively, a factor of 10 increase could be expected compared to the field in the symmetric arrangement shown in Fig. 5b [50]. It is noteworthy that the relative position of the nanoparticle with respect to the membrane could be controlled via the nanoparticle's surface functionalization [51-55]. There are bio-reagents, e.g., antibodies, which can be used to assure a specific target location.

By the design, MENPs have an effect on opening ion channels to control flows of Na^+ ions. When a neuron receives an electrical signal generated by MENPs in response to application of a magnetic field, local channels open (or close, depending on the applied magnetic field's spatiotemporal pattern conditions), allowing mostly sodium ions to cross the membrane, leading the membrane's local depolarization. This depolarization may result in activation (or inhibition) of an action potential, thus transmitting (or blocking) a signal to other neurons. Hence, MENPs represent a powerful tool to control inter-neuronal communication in neural networks.

(a)

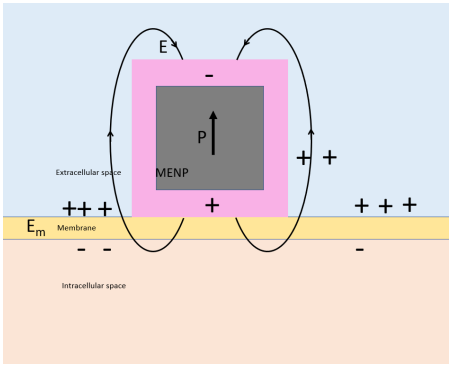

(b)

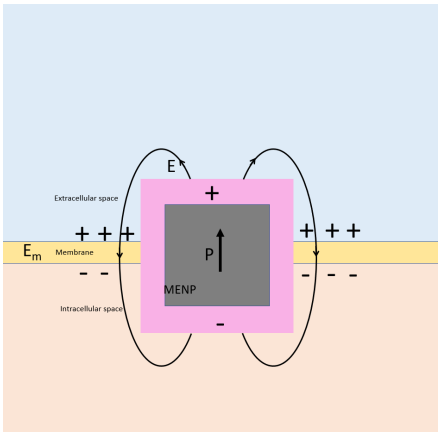

Fig. 5. (a) Illustration of an alternative arrangement when the nanoparticle is in extracellular space. (b) Illustration of a symmetric arrangement of a MENP with respect to the membrane. Depending on the permeability of the membrane, other arrangements are also possible.

In this study, two hypothetical cases are considered depending on the above two relative symmetry positions of MENPs with respect to the membrane surface. According to the first case, MENPs do not penetrate neurons but rather stick to the membrane surface and control channels to affect the firing rate. This is shown in **Fig. 6 (a)**, where the MENPs remain in the extracellular space. **Fig. 7 (a)** depicts the proposed circuit model for this scenario, and the equation governing the model is the same as **Eq. 3** with I_{ext}'**.** As can be seen, the circuit includes MENPs as an external source which can increase the total external a.c. current. If the net external current caused by MENPs increases, it will increase the inward current through these channels. In turn, this will result in depolarization of the membrane potential, as it adds to the sodium current and counteracts the potassium current.

In the second case, MENPs cross the membrane, thus inducing a stronger electric field variation across the membrane. In turn, their magnetically controlled electric fields could significantly alter electrical properties of the membrane, thus leading to visible changes in the membrane potential and excitability of the neuron, potentially causing it to fire more easily and with greater frequency. The configuration with nanoparticles crossing the membrane is suggested because the field strength across the membrane in this case is approximately a factor of two larger, in turn leading to a more effective modulation process, compared to the other configuration under study. **Fig. 6 (b)** illustrates this mechanism, with the MENP entering the cell and forming channels. **Fig. 7 (b)** shows the proposed circuit model for the second theory.

In the model, MENPs' nonlinear conductance is denoted by the symbol g'_{th} ($= \eta / Z_{th}$, η is a constant) which is used to represent the MENPs channel. The voltage-current equations shown below are derived from a mathematical analysis of the equivalent circuit:

$$C_m\left(\frac{dV(t,x)}{dt}\right) = I'_{ext}(t,x) - g_{Na}(V - V_{Na}) - g_K(V - V_K) - g_L(V - V_L) - g_{th}(V - V_{th}) = I'_{ext}(t,x) - \sum I_i(t,x) - \boldsymbol{I_{MENPs}(t,x)} \quad (14)$$

$$I_{ion=} \sum I_i(t,x) + \sum g_i(V - V_i) \quad (15)$$

As a result, the model consists of four major ion channels: sodium (Na^+), potassium (K^+), leak (L), and MENPs, in which g'_{th} is MENPs conductance and its reversal potentials is E_{th} ($V_{th} = E_{th} - E_r$, where E_r is the absolute value of the resting potential). In the HH spiking model, the gate-controlled variables n, m, h, and δ determine the conductance value of each ion channel. Based on eq. 14, when the conductance of the MENPs channels increases, the term $g_{th}(V - V_{th})$ will have a larger contribution to the equation. Depending on the value of V_{th}, if the equilibrium potential for MENPs ions is closer to the resting membrane potential (V), an increase in the conductance of the MENPs channels can further enhance depolarization, leading to increased excitability and potentially altering the firing properties of the neuron.

The effect of MENPs can be modeled as a memristive device in which the relationship between the charge passing through the MENPs and the resulting flux linkage can be modeled. The charge passing through the MENPs can be related to the magnetic field strength or other relevant parameters. The flux linkage can represent the resulting local electric fields generated by the MENPs, which in turn influence the behavior of ion channels.

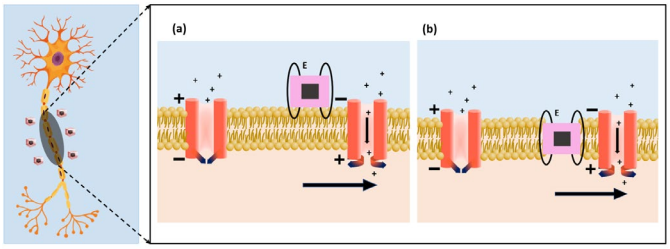

Fig. 6. (a) MENPs' impact on neuron cell and (b) (imaginary) effect of generating current flow in the longitudinal direction.

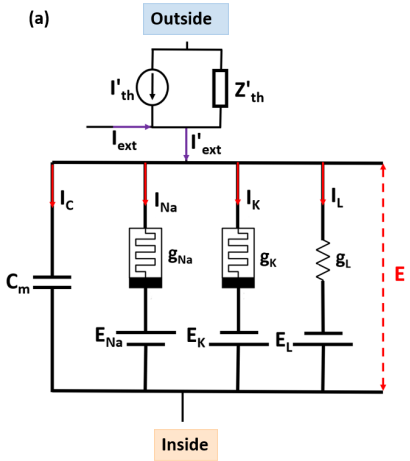

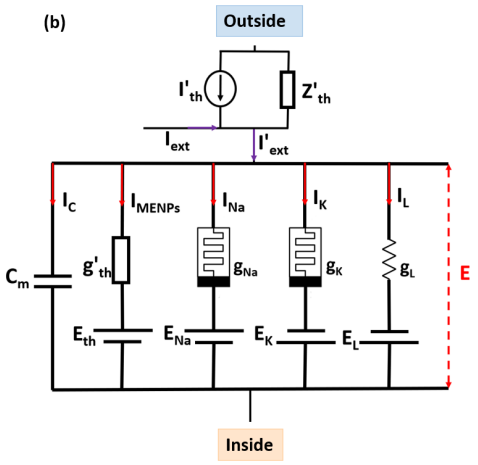

Fig.7. MENPs memristive Hodgkin-Huxley (MMHH) Model circuit representation of the effect of MENPs on neuronal membrane.

Furthermore, when MENPs are integrated into the memristor-like system, they bring an additional memory feature because of their magnetic anisotropy property. This magnetic anisotropy is due to the quantum-mechanical magneto-crystalline anisotropy of the core material, due to the electron spin-orbit coupling in cobalt ferrite – the material used as the core in the most traditional core-shell configuration such as the $CoFe_2O_4$@$BaTiO_3$. Cobalt ferrite has a magnetocrystalline anisotropy of approximately 10^6 J/m^3, which in turn implies that if nanoparticles with a characteristic size of above 10 nm are magnetized, they remain magnetized for at least a few days, in other words, have a memory property. In turn, due to the magnetoelectric effect of this nanoparticle system, this memory property can be controlled via application of a magnetic field. Hence, this memory property can be finely tuned via control of nanoparticles' intrinsic properties. In summary, the origin of the memristive-device-like property is two-fold: (1) sodium and potassium channel conductance and (2) the magneto-crystalline anisotropy of MENPs.

The most straightforward approach would be to assume a uniform distribution of nanoparticles over the membrane surface, at least in piecewise approximation. The number of neurons necessary to depolarize the membrane and trigger firing depends on various factors, including nanoparticle density, neuronal sensitivity to external stimuli, and experimental conditions. Typically, a critical threshold of neuronal activation needs to be surpassed to initiate firing, but the precise number of neurons required can vary widely based on these factors. In turn, this threshold scales with the effective number of ion channels.

The density of ion channels, denoted as X/cm^2, represents the number of ion channels present per unit area of the neuronal cell membrane. Ion channels play a crucial role in regulating the flow of ions, such as sodium, potassium, and calcium, across the cell membrane, thereby influencing neuronal excitability and signaling. The density of ion channels in neurons can vary depending on the specific type of ion channel, the neuronal population, and the region of the brain. It is challenging to provide a single specific number for ion channel density in

neurons as it can differ across various studies and neuronal subtypes.

It is also important to note that the density of MENPs, A, should be considered in relation to the density of ion channels, B, with the goal to gauge the magnitude of MENPs' effects on neuron activity. When MENPs' density is significantly smaller than the density of ion channels, i.e., A << B, the observed effect would be relatively weak. Conversely, when MENPs' density is comparable to or approximately equal to the density of ion channels, i.e., A~ B, the effect becomes more pronounced, leading to a more substantial modulation of neuron activity. A reasonable estimation for A and B to provide an adequate modulation level of neuronal activity could be in the range of 1×10^{11} to 1×10^{9} ion channels per cm^2 [56-62]. It is important to note that the specific values for A and B can vary depending on the neuron type, brain region, and experimental conditions.

Furthermore, in order to incorporate noise into the MMHH model, a set of differential equations can be used to describe how ion channels open and close in response to membrane potential in the presence of MENPs. A stochastic term can be added to the differential equations that describe how the gating variables, which control when the ion channels open and close, act to include noise in the model. This random term is shown by a random variable called ζ(t), which has the properties of white noise, which means that it has no mean and is delta-correlated. The stochastic term allows the model to better capture the variability and randomness in real-world neuron behavior, which is important for understanding how the brain processes information and generates complex behaviors.
The stochastic term would be added using the following equations:

$$\frac{dX}{dt} = \alpha_X(1 - X) - \beta_X X + \sigma'_X \zeta_X(\mathrm{t}) \qquad (16)$$

where X represents one of the gating variables (n, m, h, δ), α and β are functions that describe the opening and closing rates of the ion channel, σ' is a function that describes the strength of the noise, and ξ(t) is the white noise term. The noise amplitudes can be chosen based on the amount of noise in the experimental data, or they can be estimated from the data using methods like maximum likelihood estimation [63] or Bayesian inference [43, 64]. Adding noise to the model can account for the fact that neurons don't always act the same way and can explain things like stochastic resonance, where the presence of noise can change the response of a neuron to a weak signal. However, it can also make the model more complicated and make it harder to look at and understand the results.

III. Conclusion

This paper describes a novel physical neuron model that incorporates MENPs and calculates their effects to control neural activity via application of magnetic fields. The study emphasizes MENPs' ability to locally modulate neuron activity in a non-invasive and wireless manner. In turn, this has two major implications. First, MENPs' properties, e.g., their magnetoelectric effect, saturation magnetization, size, shape, density and localization regions, and the applied magnetic field's spatiotemporal profiles can be optimized to provide the required local modulation of neural activity in a wireless and non-invasive manner. Such analog circuits can be used to model both single-cell and collective effects in nervous systems. Second, the ability of MENPs to locally modulate neural activity has implications for the development of therapies for a variety of neurological disorders. Unlike the current DBS technology, MENPs approach does not use any surgically invasive electrodes. Unlike optogenetics - the current state of the art in research in the field of neuroscience – MENPs do not require genetic modification or surgery to introduce light activation, especially in the blue end of the optical spectrum [65]. In this study, a MENPs-based Memristive HH Model circuit has been developed that describes the effect of MENPs on neurons. In order to provide an insight into neuron's behavior in response to external stimuli such as an electric field generated by MENPs via application of a magnetic field, several key circuit equations are derived, and two analog circuit models are analyzed using the principles of ion channel activation and inactivation.

Funding

This research was partially supported by the National Science Foundation (NSF) under award #ECCS-211082 and the Defense Advanced Research Projects Agency (DARPA) and Naval Information Warfare Center, Pacific (NIWC Pacific) under Contract N66001-19-C-4019.

Declarations

The authors declare no conflict of interest.

References

1. Khizroev, S. and P. Liang, *Engineering future medicines with magnetoelectric nanoparticles: wirelessly controlled, targeted therapies.* IEEE Nanotechnology Magazine, 2019. **14**(1): p. 23-29.
2. Zhang, E., et al., *Magnetic-Field-Synchronized Wireless Activation of Action Potentials by Magnetoelectric Nanoparticles.*
3. Yue, K., et al., *Magneto-Electric Nano-Particles for Non-Invasive Brain Stimulation.* Plos One, 2012. **7**(9).
4. Zhang, E., et al., *Magnetic- field-synchronized wireless modulation of neural activity by magnetoelectric nanoparticles.* Brain Stimulation, 2022. **15**(6): p. 1451-1462.

5. Wang, P., et al., *Colossal Magnetoelectric Effect in Core-Shell Magnetoelectric Nanoparticles.* Nano Letters, 2020. **20**(8): p. 5765-5772.
6. Wang, P., et al., *Scanning probe microscopy study of cobalt ferrite-barium titanate coreshell magnetoelectric nanoparticles.* Journal of Magnetism and Magnetic Materials, 2020. **516**.
7. Raimondo, J.V., et al., *Ion dynamics during seizures.* Frontiers in Cellular Neuroscience, 2015. **9**.
8. Bédard, C. and A. Destexhe, *A modified cable formalism for modeling neuronal membranes at high frequencies.* Biophysical journal, 2008. **94**(4): p. 1133-1143.
9. Harnett, M.T., et al., *Potassium channels control the interaction between active dendritic integration compartments in layer 5 cortical pyramidal neurons.* Neuron, 2013. **79**(3): p. 516-529.
10. Yarom, Y. and J. Hounsgaard, *Voltage fluctuations in neurons: signal or noise?* Physiological reviews, 2011. **91**(3): p. 917-929.
11. Gold, C., et al., *On the origin of the extracellular action potential waveform: a modeling study.* Journal of neurophysiology, 2006. **95**(5): p. 3113-3128.
12. Zhang, E., et al., *Magnetic-field-synchronized wireless modulation of neural activity by magnetoelectric nanoparticles.* Brain Stimulation, 2022. **15**(6): p. 1451-1462.
13. Marrella, A., et al., *Magnetoelectric nanoparticles shape modulates their electrical output.* Frontiers in Bioengineering and Biotechnology, 2023. **11**.
14. Fiocchi, S., et al., *Modelling of magnetoelectric nanoparticles for non-invasive brain stimulation: a computational study.* Journal of Neural Engineering, 2022. **19**(5): p. 056020.
15. Bok, I., et al., *In silico assessment of electrophysiological neuronal recordings mediated by magnetoelectric nanoparticles.* Scientific Reports, 2022. **12**(1): p. 8386.
16. Yue, K., et al., *Magneto-electric nano-particles for non-invasive brain stimulation.* 2012.
17. Elric Zhang, P.L., Yagmur Akin Yildirim, Shawnus Chen, Mostafa Abdel-Mottaleb, Max Shotbolt, Zeinab Ramezani, Jieyuan Tian, Victoria Andre, Sakhrat Khizroev, *Ab Initio Physics Considerations in The Design of Wireless and Non-invasive Neural Recording Systems Using MagnetoElectric Nanoparticles.* IEEE Transactions on Magnetics, 2023. **59**(10): p. 1-5.
18. Bruce, A., *Molecular biology of the cell*. 1983: Garland publishing.
19. Hille, B., *Ion Channels of Excitable Membranes Third Edition.* (No Title), 2001.
20. Hodgkin, A.L. and A.F. Huxley, *A quantitative description of membrane current and its application to conduction and excitation in nerve.* The Journal of physiology, 1952. **117**(4): p. 500.
21. Neher, E. and B. Sakmann, *Single-channel currents recorded from membrane of denervated frog muscle fibres.* Nature, 1976. **260**(5554): p. 799-802.
22. Gouwens, N.W., et al., *Systematic generation of biophysically detailed models for diverse cortical neuron types.* Nature communications, 2018. **9**(1): p. 710.
23. Ramaswamy, S., *Data-driven multiscale computational models of cortical and subcortical regions.* Current opinion in neurobiology, 2024. **85**: p. 102842.
24. Teeter, C., et al., *Generalized leaky integrate-and-fire models classify multiple neuron types.* Nature communications, 2018. **9**(1): p. 709.
25. Hawrylycz, M., et al., *Inferring cortical function in the mouse visual system through large-scale systems neuroscience.* Proceedings of the National Academy of Sciences, 2016. **113**(27): p. 7337-7344.
26. Alexandersen, C.G., et al., *A multi-scale model explains oscillatory slowing and neuronal hyperactivity in Alzheimer's disease.* Journal of the Royal Society Interface, 2023. **20**(198): p. 20220607.
27. Gratiy, S.L., et al., *BioNet: A Python interface to NEURON for modeling large-scale networks.* PLoS One, 2018. **13**(8): p. e0201630.
28. Smith, I.T., et al., *Nanomedicine and nanobiotechnology applications of magnetoelectric nanoparticles.* Wiley Interdisciplinary Reviews-Nanomedicine and Nanobiotechnology, 2022.
29. Nair, M., et al., *Externally controlled on-demand release of anti-HIV drug using magneto-electric nanoparticles as carriers (vol 4, pg 1707, 2013).* Nature Communications, 2013. **4**.
30. Stewart, T., et al., *Magnetoelectric particles cross blood brain barrier to deliver anti-tumor*

peptide to glioblastoma cells with on-demand release. Cancer Research, 2016. **76**.
31. Rodzinski, A., et al., *Targeted and controlled anticancer drug delivery and release with magnetoelectric nanoparticles.* Scientific Reports, 2016. **6**.
32. Purves, D., et al., *Circuits within the basal ganglia system*, in *Neuroscience. 2nd edition*. 2001, Sinauer Associates.
33. Hille, B., *Ion channels of excitable membranes. Sunderland, MA, USA: Sinauer Assoc.* Inc. Publishers, 2001. **813**.
34. Levitan, I.B. and L.K. Kaczmarek, *The neuron: cell and molecular biology*. 2002: Oxford University Press, USA.
35. Mannan, Z.I., et al., *Memristive imitation of synaptic transmission and plasticity.* IEEE transactions on neural networks and learning systems, 2019. **30**(11): p. 3458-3470.
36. Hines, M.L. and N.T. Carnevale, *Translating network models to parallel hardware in NEURON.* Journal of neuroscience methods, 2008. **169**(2): p. 425.
37. Hodgkin, A.L. and A.F. Huxley, *Currents carried by sodium and potassium ions through the membrane of the giant axon of Loligo.* The Journal of physiology, 1952. **116**(4): p. 449.
38. Beck, M.E., et al., *Spiking neurons from tunable Gaussian heterojunction transistors.* Nature communications, 2020. **11**(1): p. 1565.
39. Hegab, A.M., et al., *Neuron model with simplified memristive ionic channels.* International Journal of Bifurcation and Chaos, 2015. **25**(06): p. 1530017.
40. Chua, L., V. Sbitnev, and H. Kim, *Hodgkin–Huxley axon is made of memristors.* International Journal of Bifurcation and Chaos, 2012. **22**(03): p. 1230011.
41. Chua, L., *If it's pinched it'sa memristor.* Semiconductor Science and Technology, 2014. **29**(10): p. 104001.
42. Ramezani, Z. and A. Ahmadivand, *Fundamental Phenomena in Nanoscale Semiconductor Devices*, in *Sub-Micron Semiconductor Devices*. 2022, CRC Press. p. 1-22.
43. Xu, W., J. Wang, and X. Yan, *Advances in memristor-based neural networks.* Frontiers in Nanotechnology, 2021. **3**: p. 645995.
44. Chua, L., *Memristor-the missing circuit element.* IEEE Transactions on circuit theory, 1971. **18**(5): p. 507-519.
45. Chua, L.O. and S.M. Kang, *Memristive devices and systems.* Proceedings of the IEEE, 1976. **64**(2): p. 209-223.
46. Yang, X. and H. He, *Adaptive critic designs for optimal control of uncertain nonlinear systems with unmatched interconnections.* Neural Networks, 2018. **105**: p. 142-153.
47. Izhikevich, E.M., *Dynamical systems in neuroscience*. 2007: MIT press.
48. Pikovsky, A., et al., *A universal concept in nonlinear sciences.* Self, 2001. **2**: p. 3.
49. Kozielski, K.L., et al., *Nonresonant powering of injectable nanoelectrodes enables wireless deep brain stimulation in freely moving mice.* Science advances, 2021. **7**(3): p. eabc4189.
50. Stimphil, E., et al., *Physics considerations in targeted anticancer drug delivery by magnetoelectric nanoparticles.* Applied Physics Reviews, 2017. **4**(2).
51. Tallawi, M., et al., *Strategies for the chemical and biological functionalization of scaffolds for cardiac tissue engineering: a review.* 2015. **12**(108): p. 20150254.
52. Liebana, S. and G.A.J.E.i.b. Drago, *Bioconjugation and stabilisation of biomolecules in biosensors.* 2016. **60**(1): p. 59-68.
53. Goossens, J., et al., *Functionalization of gold nanoparticles with nanobodies through physical adsorption.* 2017. **9**(23): p. 3430-3440.
54. Parracino, M.A., B. Martín, and V. Grazú, *State-of-the-art strategies for the biofunctionalization of photoactive inorganic nanoparticles for nanomedicine*, in *Photoactive Inorganic Nanoparticles*. 2019, Elsevier. p. 211-257.
55. Gordon, M.R., et al., *Field guide to challenges and opportunities in antibody–drug conjugates for chemists.* 2015. **26**(11): p. 2198-2215.
56. Goldin, A.L., *Resurgence of sodium channel research.* Annual review of physiology, 2001. **63**(1): p. 871-894.
57. Hille, B., *Ionic channels in excitable membranes. Current problems and biophysical approaches.* Biophysical journal, 1978. **22**(2): p. 283-294.
58. Hille, B.v. *Ionic channels of excitable membranes*. 2001.
59. Llinás, R.R., M. Sugimori, and B. Cherksey, *Voltage-dependent calcium conductances in mammalian neurons: The P channel.* Annals of the New York Academy of Sciences, 1989. **560**(1): p. 103-111.

60. Traynelis, S.F., et al., *Glutamate receptor ion channels: structure, regulation, and function.* Pharmacological reviews, 2010. **62**(3): p. 405-496.
61. Olsen, R.W. and W. Sieghart, *International Union of Pharmacology. LXX. Subtypes of γ-aminobutyric acidA receptors: classification on the basis of subunit composition, pharmacology, and function. Update.* Pharmacological reviews, 2008. **60**(3): p. 243-260.
62. Nilius, B. and A. Szallasi, *Transient receptor potential channels as drug targets: from the science of basic research to the art of medicine.* Pharmacological reviews, 2014. **66**(3): p. 676-814.
63. Pan, J.-X., et al., *Maximum likelihood estimation.* Growth curve models and statistical diagnostics, 2002: p. 77-158.
64. Box, G.E. and G.C. Tiao, *Bayesian inference in statistical analysis*. 2011: John Wiley & Sons.
65. Chen, R., et al., *Deep brain optogenetics without intracranial surgery.* Nature Biotechnology, 2021. **39**(2).